Analysis of Ocean Wave Energy-Driven Desalination Methods for Sustainable Water Production

A thesis proposal presented to the faculty of the Graduate School of Western Carolina University in partial fulfillment of the requirements for the degree of Master of Science in Engineering Technology

By
Irfanul Hasan

Director: Dr. Bora Karayaka
Professor
School of Engineering + Technology

Committee Members:
Dr. Yi-Hsiang Yu, School of Engineering + Technology
Dr. Tarek Kandil, School of Engineering + Technology

December 2024

ACKNOWLEDGEMENTS

I am incredibly proud to be part of Western Carolina University. The faculty members have provided immense support throughout my journey toward attaining my degree, enriching my knowledge and fueling my enthusiasm for learning.

I would especially like to thank Dr. Bora Karayaka for his invaluable guidance in my research. He introduced me to the field of ocean wave energy converters and desalination, and I consider myself fortunate to have had the opportunity to work with him. His dedication to research has inspired me to give my best effort in all my work. Dr. Karayaka's friendly and supportive nature has been a tremendous blessing, and I am grateful to have him as my thesis supervisor.

I also want to extend my thanks to my committee members, Dr. Tarek Kandil and Dr. Yi-Hsiang Yu, for their collaboration and contribution to my research. Additionally, I am grateful to my graduate classmates for their assistance and friendship throughout this journey.

Lastly, I want to express my heartfelt thanks to my family for their patience, love, and unwavering support.

LIST OF TABLES

LIST OF FIGURES

ABSTRACT

ANALYSIS OF OCEAN WAVE ENERGY-DRIVEN DESALINATION METHODS FOR SUSTAINABLE WATER PRODUCTION

Irfanul Hasan, MSET

Western Carolina University (December 2024)

Director: Dr. Bora Karayaka

This thesis investigates the potential of wave energy to drive a desalination system for sustainable water production, addressing the increasing need for innovative solutions to global water scarcity. Initially, simulation studies are conducted using the oscillating surge wave energy converter (OSWEC) system to generate the high-pressure flow required for reverse osmosis (RO) desalination. The OSWEC system, developed by the National Renewable Energy Laboratory (NREL), serves as a benchmark. These experiments explore the effects of varying the number of parallel membranes, piston areas, and sea states on permeate flow and water salinity. A strong correlation is found between permeate flow and piston area. A positive correlation is also observed between permeate flow and membrane quantity; however, this correlation diminishes after reaching a saturation point. This foundational work provides key insights into optimizing desalination system performance. Building on these results, the research further develops an ocean wave energy-driven electrical desalination plant, utilizing a floating buoy and spar coupled with a slider crank mechanism to convert wave energy into electrical power. The system is equipped with a maximum power point tracking (MPPT) control algorithm, which drives a rotary positive displacement pump to enhance RO efficiency. To maximize freshwater production, the study focuses on electrical power generation for desalination rather than offshore water pumping. The desalination system RO membrane model at this stage is developed based on simulation experiments from the OSWEC benchmark system. Six sea states are selected to represent different deployment conditions along the U.S. West Coast, yielding a maximum permeate flow rate in the range of 155 to 225 gallons per minute. This project advances renewable energy applications for desalination, offering eco-friendly solutions to water scarcity while aligning with global sustainable development goals.

CHAPTER 1: INTRODUCTION AND LITERATURE REVIEW

Over 70% of Earth's surface is covered by water, and approximately 80% of the global population resides in coastal regions [1]. However, over 97% of this water is saline, rendering it unsuitable for drinking, agriculture, and most industrial applications [2]. According to the United Nations, a child dies from water-related issues every nine minutes, and by 2050, more than 2 billion people across 50 countries are projected to face severe water shortages [3]. In the United States alone, approximately one million residents in California are exposed to contaminated water annually, with freshwater supply shortages anticipated in around 40 states in the coming decades [4].

To tackle the growing challenge of water scarcity and ensure water security, desalination has emerged as a promising alternative for freshwater production. Among desalination technologies, reverse osmosis (RO) stands out as a widely adopted method due to its pressure-driven separation process using semi-permeable membranes, offering high energy efficiency and proven technical reliability [5]. Despite its potential, most RO-based seawater desalination plants rely on fossil fuels for energy, contributing to significant carbon emissions. This reliance not only raises sustainability concerns but also exacerbates climate change [6].

Water scarcity remains one of the most pressing global challenges, with billions of people facing limited access to water for at least part of the year, particularly in regions prone to droughts and water stress [7]. Remote rural areas, such as islands, are especially vulnerable to these shortages [8]. Additionally, industries and energy production often depend on large quantities of clean water to function effectively [9]. Ensuring access to clean water is essential for sustainable development, driving social, economic, and environmental progress.

Recent advancements in desalination technology have focused on integrating renewable energy sources for enhanced sustainability. Mi et al. conducted an experimental investigation of a mechanically driven reverse osmosis (RO) desalination system powered by wave energy [10]. Figure 1.1 illustrates the schematic setup of their experiment.

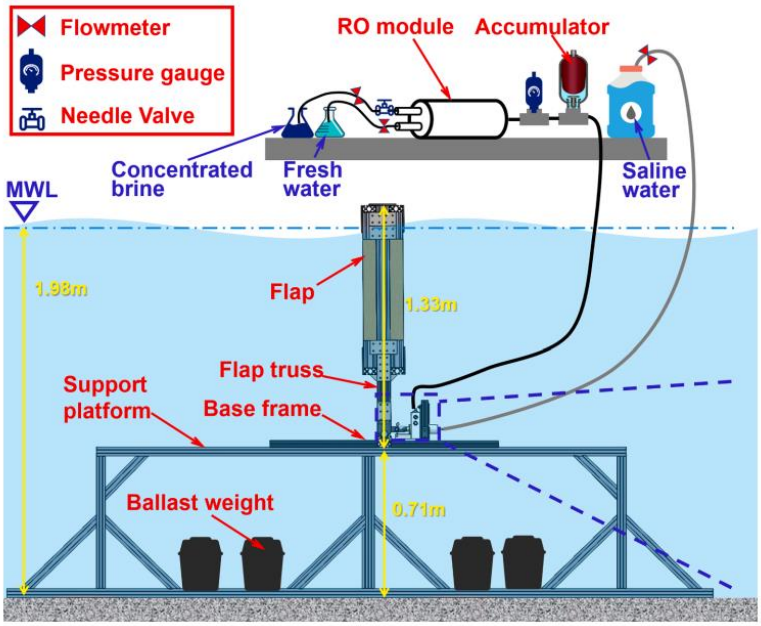

Figure 1.1: Schematic of the experiment setup [10]

This system uses an oscillating surge wave energy converter (OSWEC) to drive a piston pump, pressurizing seawater for desalination. Key components include an accumulator to mitigate pressure fluctuations and a needle valve to adjust system pressure and water recovery. Testing a 1:10 scale model in a wave tank demonstrated significant improvements in specific water productivity, highlighting the potential for sustainable desalination. The study presents several advantages, including the innovative use of abundant wave energy and reduced fossil fuel dependency. However, challenges include managing pressure fluctuations in variable wave conditions and ensuring the durability of mechanical components in harsh marine environments.

While the scaled model results are promising, further research is needed to evaluate the feasibility and efficiency of full-scale deployments.

In a comprehensive review by Jennifer Leijon and Cecilia Boström, the potential of wave-powered desalination as a sustainable solution to global freshwater scarcity was examined [11]. The thesis explored desalination techniques like reverse osmosis, electrodialysis, and mechanical vapor compression for integration with wave energy converters (WECs), detailing key WEC types such as oscillating water columns, oscillating bodies, and overtopping systems. Successful projects like Delbuoy, CETO Freshwater, and SAROS have demonstrated the feasibility of wave-powered desalination. The review acknowledged environmental and technical challenges, including intermittency in power generation and the cost-effectiveness of produced water. Leijon and Boström emphasized the need for advanced control systems, hybrid renewable energy solutions, and improved integration into existing water supply infrastructures. While highlighting the promise of wave-powered desalination, the review identified critical gaps in commercialization and scalability, calling for robust research efforts to overcome technological barriers and ensure economic viability in diverse coastal settings worldwide.

Yu et al. explored integrating an oscillating surge wave energy converter (OSWEC) with reverse-osmosis (RO) desalination in their study on wave-powered desalination systems (WPDS) [12]. They used a comprehensive wave-to-water numerical model combining WEC-Sim for hydrodynamic simulations and a solution-diffusion model for RO processes. The approach evaluated the feasibility of generating freshwater from wave energy, validated against empirical data and the ROSA model. The study effectively predicted system performance under varying wave conditions, offering insights into managing hydraulic fluctuations through strategies like pressure accumulators and relief valves. However, it included check valves for flow regulation and

did not integrate Maximum Power Point Tracking (MPPT). Yu and Jenne's work advances understanding in wave-powered desalination, but future research should explore integrating MPPT and optimizing hydraulic stability with check valves to enhance WPDS efficiency and reliability.

The research by R. Suchithra et al. outlined a compact and modular wave-powered desalination system influenced by US DOE Waves to Water competition rules [13]. Their approach used an OSWEC flap-type wave surge converter to generate hydraulic piston force, driving a desalination process through a double-acting cylinder and RO module. Numerical tools like WEC-Sim and MATLAB simulate system performance under different sea states, achieving 50 bar seawater feed pressure and up to 100 L/h freshwater with total dissolved solid (TDS) levels below 500 mg/L. An accumulator mitigates pressure fluctuations, enhancing stability. Strengths include innovative energy capture and detailed performance validation, while challenges include the absence of MPPT and usage of check valves. Scalability and adaptability to diverse conditions require further exploration to ensure robust performance.

Recent advancements in renewable energy have spurred interest in ocean-wave-powered reverse osmosis (RO) desalination systems. Mi et al. developed an innovative Ocean Surface Wave Energy Converter (OSWEC) with a double-acting piston pump that efficiently converted bidirectional wave motion into unidirectional hydraulic energy for RO desalination [14]. Figure 1.2 illustrates the overall schematic of their proposed ocean-wave-powered desalination system.

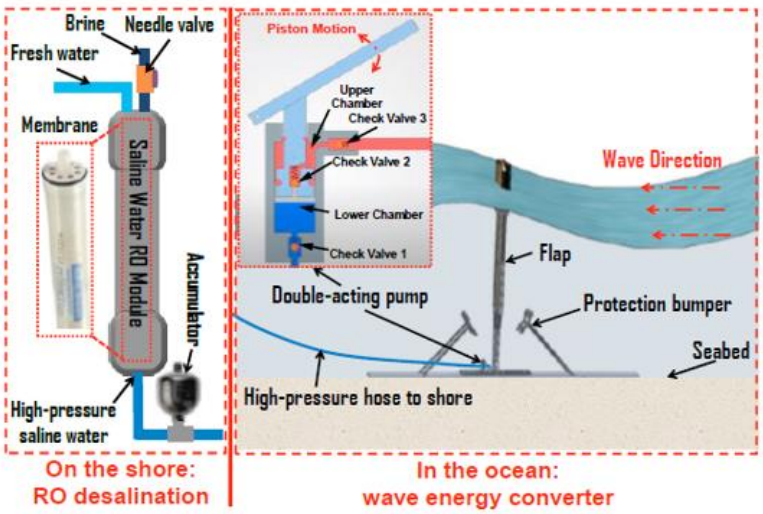

Figure 1.2: Overall schematic of the proposed ocean wave powered desalination system [14]

They integrated a spring ball-based check valve to enhance fluid flow control and minimize energy losses, optimizing system efficiency. Although lacking MPPT for wave energy extraction, Mi et al. validated their concept through numerical modeling and wave tank tests, demonstrating promising energy conversion efficiency and desalination performance across varying wave conditions. This approach, combining simulations with practical experiments, underscored the system's scalability and potential in real-world applications. By harnessing wave energy directly at sea, this technology reduces reliance on fossil fuels, offering a sustainable solution to water scarcity challenges and promoting environmental resilience in coastal areas.

Leijon et al. studied using ocean wave energy to power reverse osmosis (RO) desalination in Kilifi, Kenya, focusing on integrating a Rainman desalination system with wave and solar power [15]. Their experimental setup assessed RO system performance under variable wave energy typical of Kilifi's coastal conditions in 2015. Results showed wave energy's potential to sustain RO operations, despite fluctuations, although freshwater production varied below peak capacity. Strategies proposed to mitigate variability included energy storage and additional converters.

Hybrid wave-solar systems were explored for enhanced output, highlighting the need for further research in optimizing wave-powered RO for coastal communities.

In recent years, ensuring stable freshwater supply has become critical for island communities like Gotland, Sweden. Wave energy offers a promising solution by powering an electrically driven desalination plant using RO technology. WECs convert ocean wave energy into electricity, with Gotland's estimated annual wave energy potential of 1891 MWh capable of meeting the desalination plant's 350 MWh requirement annually. The model employed 50 WECs, each averaging 4.3 kW annually, demonstrating the effectiveness of relatively small converters. The study considers factors such as wave energy variability and conversion efficiency, noting potential enhancements through combining wave energy with solar power to ensure continuous freshwater supply even during low wave activity [16]. For shallow water deployments, such as those in the U.S. Atlantic coastal areas, WECs need to be installed at locations farther from the coast to capture usable energy. Previous studies proposed water pumping mechanisms, which are not suitable for this setting due to economic concerns.

In this thesis, the study focuses on utilizing an ocean wave energy-driven electrical desalination plant suitable for the U.S. Atlantic coast. This approach harnesses wave energy through a WEC comprising a floating buoy, spar, and slider crank mechanism. Electrical energy generated, optimized by a MPPT control algorithm, drives reverse osmosis (RO) desalination process. The objective is to develop a high-efficiency, wave-powered desalination system to address water scarcity in drought-affected regions, aligning sustainable development goals. The thesis covers an introduction on droughts, wave energy potential, a methodology using WEC-Sim for simulation, desalination system details, results analysis, and conclusions on climate change mitigation and water provision.

CHAPTER 2: METHODOLOGY

2.1 Mechanically Powered Desalination

2.1.1 Benchmark OSWEC desalination system analysis and optimization for maximum permeate flow

WEC-Sim (Wave Energy Converter SIMulator) is an open-source software for simulating wave energy converters. The software is developed in MATLAB/Simulink using the multi-body dynamics solver Simscape Multibody [17]. The OSWEC based desalination system used in this study is presented in a schematic form in Figure 2.1.

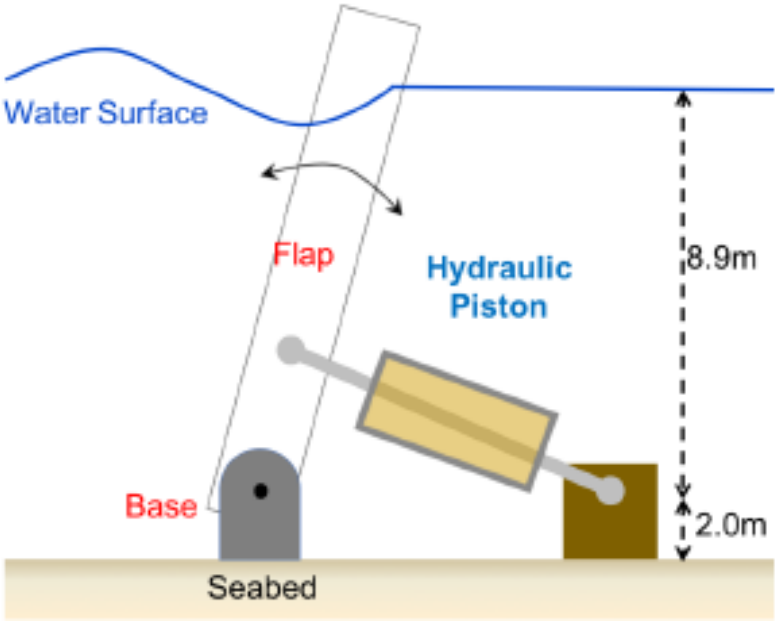

Figure 2.1: The schematic representation of the OSWEC [12]

The sea states were selected following the methodology used in the Wave Energy Prize study, which considered six sea states for a specific region on the U.S. west coast, as shown in Table 2.1 [12].

Table 2.1: Selected Wave Environment

Sea State, SS#	Peak Period, T_p(s)	Significant Wave Height, H_s (m)
SS1	7.31	2.34
SS2	9.86	2.64
SS3	11.52	5.36
SS4	12.71	2.05
SS5	15.23	5.84
SS6	16.50	3.25

The performance of the wave-powered RO desalination system is evaluated through a wave-to-water numerical model, as illustrated in Figure 2.2 [12].

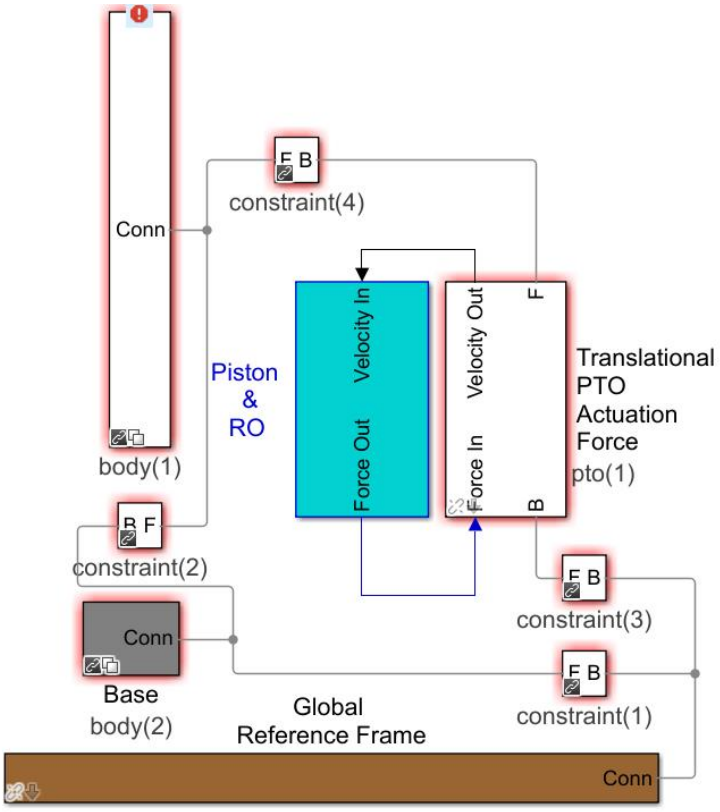

Figure 2.2: WEC-Sim wave to water model [12]

In this study, the primary objective was to maximize permeate flow in a mechanically powered desalination system, while water salinity was carefully maintained within safe, drinkable limits. Specifically, the aim was to keep salinity below the widely accepted threshold of 500 parts per million (ppm), beyond which water is generally considered unsuitable for drinking. To achieve maximum permeate flow, two key system parameters were adjusted. The first parameter, the piston area of the hydraulic pump, was progressively increased, starting with an initial area of 0.208 m^2 and then testing areas of 0.234 m^2, 0.26 m^2, 0.273 m^2, 0.286 m^2, 0.321 m^2, and 0.338 m^2. The second parameter, the membrane quantity in the system, was also adjusted.

The number of membranes was incrementally increased from 25 through a series of values: 50, 100, 183, 500, 1000, 2000, 4000, 8000, 16000, and finally to 32000 membranes. In the initial phase of the experiment, a baseline was set using 183 membranes and a piston area of 0.26 m^2. In the results and discussion section, we provide detailed analyses of the permeate flow rate trends as affected by varying piston areas and membrane quantities. To clearly illustrate these trends, the data for membrane quantities ranging from 25 to 8,000 membranes in the membrane quantity versus permeate flow rate plot is focused on.

2.1.2 Modeling and Identification of the Desalination System for the OSWEC

A WEC has the potential to convert wave energy directly into the high-pressure flow required by desalination systems to pump saltwater to RO membranes and provide the necessary pressure for freshwater generation. The proposed wave-powered desalination system utilizes an OSWEC equipped with a hydraulic piston pump to capture wave energy from the relative rotational motion between the flap and the fixed base. This desalination system is purely mechanical, as it does not involve electricity production. The OSWEC consists of a flap and a base, which are connected via a rotational joint. The flap is also linked to a linear hydraulic piston,

which converts the wave-induced torque into linear force to pump seawater through the RO membranes. The rotational motion of the OSWEC drives the hydraulic piston bidirectionally. To rectify the bidirectional motion of the piston into unidirectional hydraulic flow, a double-acting piston pump is employed. In terms of energy flow, the hydrokinetic energy from the ocean waves is captured by the OSWEC to drive the piston pump as mechanical energy. This mechanical energy is then converted into hydraulic energy, which pressurizes the seawater. The pressurized seawater is subsequently applied to the RO membrane for the filtration process. WEC-Sim is a time-domain numerical model for solving the system dynamics of WECs that consist of multiple bodies, power-take-off (PTO) systems and mooring systems [18]. The dynamic response in WEC-Sim is calculated by solving the equation of motion for each body about its center of gravity, based on Cummins' equation [19], which can be written as:

$$(m + A_\infty)\ddot{X} = -\int_0^t K(t-\tau)\,\dot{X}(\tau)d\tau + F_{exc} + F_{vis} + F_{res} + F_{EXT} + F_{mo} \qquad (1)$$

Where A_∞ is the added mass matrix at infinite frequency, X is the (translational and rotational) displacement vector of the body, m is the mass matrix, K is the matrix of impulse-response function, F_{exc}, F_{EXT}, F_{mo}, F_{vis} and F_{res} are the vector of the wave-excitation force, external force, mooring force, quadratic viscous drag term calculated using Morison's equation and net buoyancy restoring force.

To simulate the RO process, which generates permeate flow through a membrane, a solution-diffusion model was developed. The model assumes that the permeate flow Q_p is primarily dictated by the net driving pressure, which is equal to the incoming feed pressure (Δp) minus the difference in osmotic pressure ($\Delta\pi$) over the membrane [4],

$$Q_{p=}A_w A_m(\Delta p - \Delta\pi) \qquad (2)$$

where A_w is the permeability coefficient, depending on the membrane permeability, temperature and fouling factor, and A_m is the membrane active surface area. Furthermore, based on the model, the solute concentration in the permeate can be expressed as:

$$C_p = \frac{C_m}{\frac{A_w}{B_s}(\Delta p - \Delta \pi) + 1} \quad (3)$$

where C_m is the solute concentration in the membrane (seawater side) and B_s is the solute transport parameter.

The dimensions and mass properties for the OSWEC (in full scale) are listed in Table 2.2 and are given based on the values from Van't Hoff [20].

Table 2.2: Oscillating Surge Wave Energy Converter (OSWEC) Mass Properties and Dimensions: MWS, Mean Water Surface

Parameters	**Values (Unit)**
Device width and thickness	18 m x 1.8 m
Flap height	11 m
Base height	2 m
Hinge depth	8.9 m (from MWS)
Center of gravity (CG)	3.9 m (from MWS)
Water depth	10.9 m
Mass	127,000 kg
Moment of inertia (at CG)	1.85×10^6 kgm^2

The RO system typically consists of multiple pressure vessels, each containing a set of RO membranes. In some cases, multiple stages of RO membranes are arranged in series to achieve the desired water quality. These design factors influence the overall permeability of the RO system and the parameter values outlined in Equations (2) and (3). In this study, a single-pass RO system with three standard membranes (SW30HR-380) in each pressure vessel was assumed. It is also assumed that the concentration polarization effect on the membrane is negligible, simplifying the analysis.

To define the RO model and derive the necessary parameters, the water application value engine (WAVE) model was utilized. WAVE, a water-treatment design tool developed by Dow Chemical Company, is capable of evaluating a combination of RO, ultrafiltration (UF), and ion exchange (IX) water purification technologies [21]. WAVE also includes the reverse-osmosis system analysis (ROSA) model, which is used for designing and simulating RO systems. ROSA enables multistage and multi-pass calculations to determine flow, pressure, water quality, and recovery for each component in the system. In this study, the ROSA model was used to calculate the pressure and water quality before and after the membrane, as well as to determine the membrane flux for various membrane configurations and flow rates. From a manufacturing perspective, membranes are generally designed to operate within a specific pressure range, which is influenced by factors such as membrane design, the number of stages in the RO system, recovery ratio, and the number of membranes per pressure vessel. Based on the ROSA model, the membranes in this study are designed to function within a pressure range of 42–57 bar. The average values for the parameters A_w and B_s were incorporated into the RO model for this study. These values were derived by substituting Q_p and C_p, obtained from the ROSA model, into Equations (2) and (3), assuming a salinity of 35,946 ppm and an osmotic pressure of 30 bar. While these values remain nearly constant within the operational pressure range, they decrease rapidly as the pressure approaches the osmotic pressure. The averaged values of A_w and B_s used in our WEC-Sim RO model were calculated by averaging the A_w and B_s values within the designed pressure range. It is important to note that the analysis did not account for the effects of dynamic fluctuations in flow and pressure on membrane permeability and the resulting water quality. Membranes are one of the most significant cost contributors in desalination systems, encompassing both capital investment and ongoing maintenance expenses. Their economic impact is influenced by factors such as

material quality, durability, fouling resistance, and replacement frequency. Optimizing the number of membranes directly affects the system's cost efficiency; for example, fewer membranes may reduce initial costs but could lower water output or increase energy consumption due to higher operational loads. Conversely, adding membranes can enhance water production capacity and energy efficiency but raises upfront and maintenance costs. Economic considerations also include the lifespan of membranes and the associated costs of cleaning, replacement, and disposal. Innovations like advanced coatings or anti-fouling technologies can reduce these expenses over time.

2.1.3 Description of testing with 6 sea states:

The performance of the wave energy converter (WEC) was evaluated under six selected sea states, as summarized in Table 2.1 for Newport, OR. These sea states were chosen following the methodology used in the Wave Energy Prize competition, ensuring a representative range of wave conditions. The peak periods (T_p) varied between 7.31 s and 16.50 s, while the significant wave heights (H_s) ranged from 2.05 m to 5.84 m. Each WEC-Sim simulation was conducted over a 3000 s duration with a ramp-up time of 250 s to stabilize the system. A time-step size of 0.01 s was used for numerical accuracy, and the results from the final 1500 s of the simulation were considered for calculating the time-averaged performance metrics to identify RO membrane characteristics.

2.2 Electrically powered desalination

2.2.1 RM3-WEC system with slider crank Power Take Off for power generation

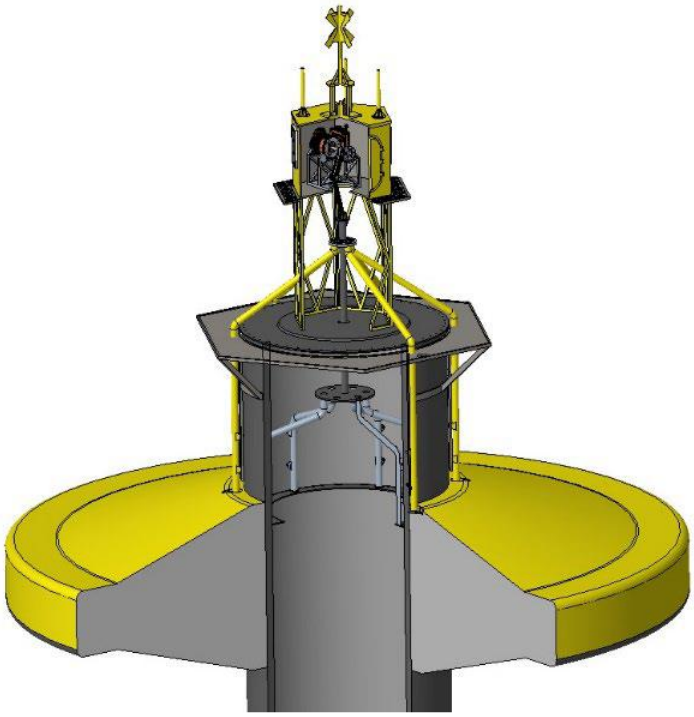

Figure 2.3: An architectural rendering of RM3 WEC system

The Reference Model 3 (RM3) is a wave point absorber, also known as a wave power buoy. The RM3 primarily captures energy from the heave motion of the float induced by incident waves. As the float oscillates, it generates electrical power. The vertical column serves as structural support and houses the necessary components for energy conversion [22]. In this research, the WEC-Sim Reference Model 3 (RM3) and Slider Crank (SC) linkage were combined, as shown in Figure 2.3, along with an electrical machine. Created in MATLAB/Simulink™, WEC-Sim utilizes Simscape Multibody R2024a for simulating multibody dynamics. This study employed the WEC-Sim RM3 model, with the hydrodynamics model configured according to [23]. To maximize solver efficiency, the SC linkage was also resolved using Simscape Multibody. A state-space (SS) model was utilized due to its requirement for a small time-step size, suitable for hardware-in-the-loop (HIL) applications; the simulation duration for the convolution formulation is significantly longer compared to the SS model.

In this setup, the stator of the electrical machine and the gearbox casing are considered fixed to the spar section. The crankshaft, rotor, and gears of the WEC-Sim RM3 are also fixed to the spar section, enabling unrestricted rotation. Meanwhile, the slider is linked to the float section, moving freely within the spar. The upward motion of the float, propelled by waves, corresponds to the slider-crank mechanism's upward stroke, assumed to rotate in a counterclockwise direction. Throughout this study, the spar section is considered fixed to the ocean floor, limiting the float section to vertical heave movement only.

2.2.2 Design of electrically powered rotational pump control system

Figure 2.4 depicts the torque production of the DC machine including the PWM DC-DC power stage block and the internal system of the phase tracking and correction process which is marked using the dashed line. The angle control algorithm is designed to optimize the performance of the WEC system by dynamically adjusting reference speed based on real-time inputs [23]. The goal of the phase tracking process is to control the speed to synchronize wave excitation force and the float velocity.

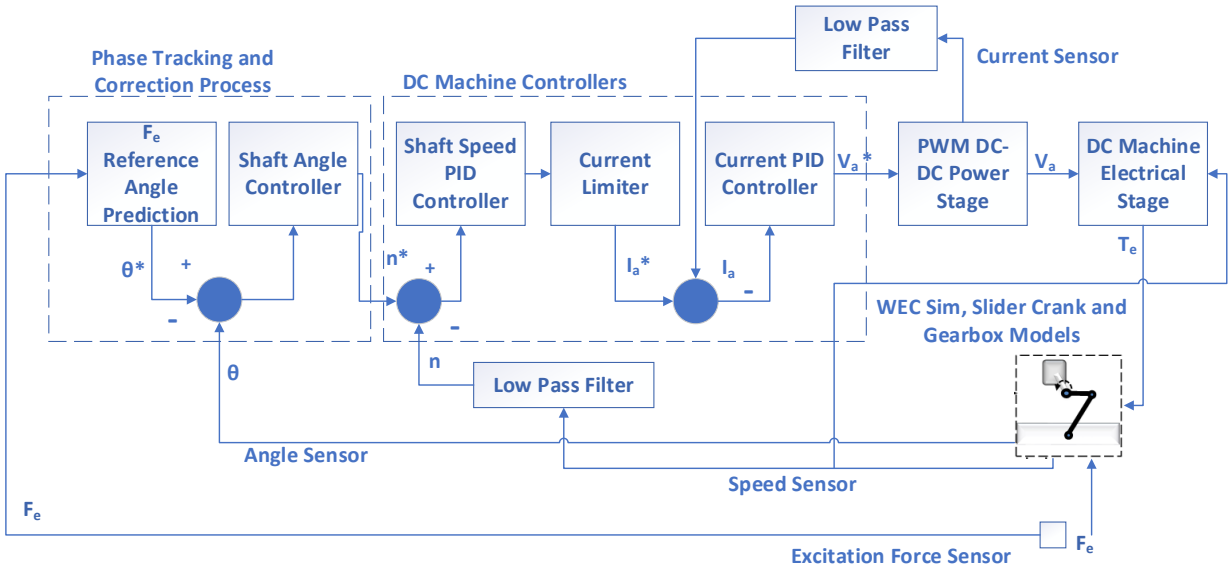

Figure 2.4: Overall MPPT control system block diagram for the numerical WEC model [23]

It is worth noting that it is crucial to synchronize the control algorithm with the wave excitation force by including several timing constants and the oscillation period of the float. The system will finally provide the optimum crankshaft shaft angle and speed. The system outputs are routed to various actuators or subsystems within the WEC which enables dynamic adjustment of the wave energy converter's parameters and ensuring optimal performance under varying conditions. Through iterative parameter tuning and real-time control, the system consistently operates near peak efficiency. Moreover, incorporating Maximum Power Point Tracking (MPPT) into the RM3 electrical desalination system significantly enhances its efficiency and reliability. MPPT ensures that the variable and often unpredictable power generated by wave energy converters is optimally utilized by continuously tracking and extracting the maximum power available. This capability is particularly crucial given the fluctuating nature of wave energy, as it reduces energy losses and improves the overall performance of the system. While MPPT involves higher costs and system complexity, its ability to adapt to dynamic wave conditions, improve energy harvesting, and enhance the economic viability of wave-powered desalination systems makes it a valuable component for sustainable water production in coastal and off-grid regions.

2.2.3 Desalination System

The primary goal at this stage is to identify an appropriate scaling factor to plan for an experimental setup within its rated parameters in the next stage of this research. A scaling factor of 15 (Sf = 15) is applied throughout the research. In the scaled-down model, the Froude scaling law is utilized to adjust various parameters, such as total flow rate and linear hydraulic resistances. For a scaling factor of 15 (Sf = 15), the total flow rate is decreased by $(Sf)^{3.5}$, while the linear hydraulic resistances are increased by $(Sf)^{3.5}$. The pressure in the reverse osmosis (RO) model remains unchanged.

Figure 2.5 illustrates a wave-powered energy system designed to drive an electrically driven desalination plant with high efficiency and reliability (see also Figure A.1 in Appendix B). The process begins with the WEC, which captures and converts ocean wave energy into electrical power, monitored continuously for optimal performance. The generated energy is then stored in a supercapacitor energy storage system, which stabilizes the power supply and ensures efficient energy management through integrated performance tracking. This stored energy is subsequently used to power an electrically driven desalination plant, employing RO technology for freshwater production. The supercapacitor (SC) size utilized in this study for the scaled-down model was selected to be 24.5 Wh. Performance and output monitoring systems are embedded to maintain seamless and reliable operation. The electrically driven desalination plant has two main components which are the RO membrane, shown in Figure 2.6 along with its electrical analogue, which is in Figure 2.7, and the speed or flow rate controller of the electrical motor, shown in Figure 2.8.

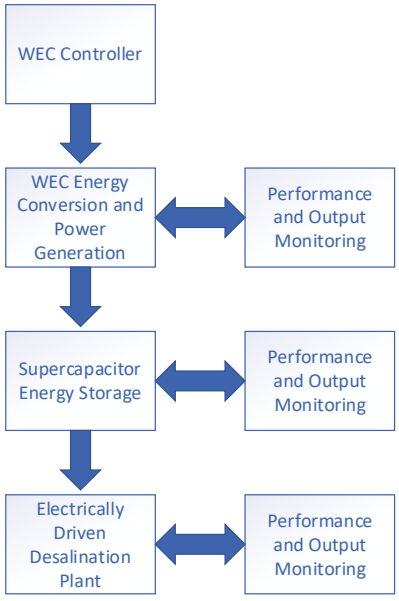

Figure 2.5: Block diagram of WEC's electric drive system with supercapacitor bank and desalination system

In Figure 2.6, the RO membrane model includes an osmotic pressure block and two linear hydraulic resistances to represent the membrane (see also Figure A.2 in Appendix B). The water flow is routed into to paths to measure both the permeate (desalinated water) output and the brine (waste) output. From a manufacturing standpoint, membranes are usually engineered to operate within specific pressure ranges, determined by factors such as membrane design, the number of RO system stages, recovery ratio, and membranes per pressure vessel. According to the RO system analysis (ROSA) model used in this study, the membranes are designed to function within a pressure range of 42–57 bar.

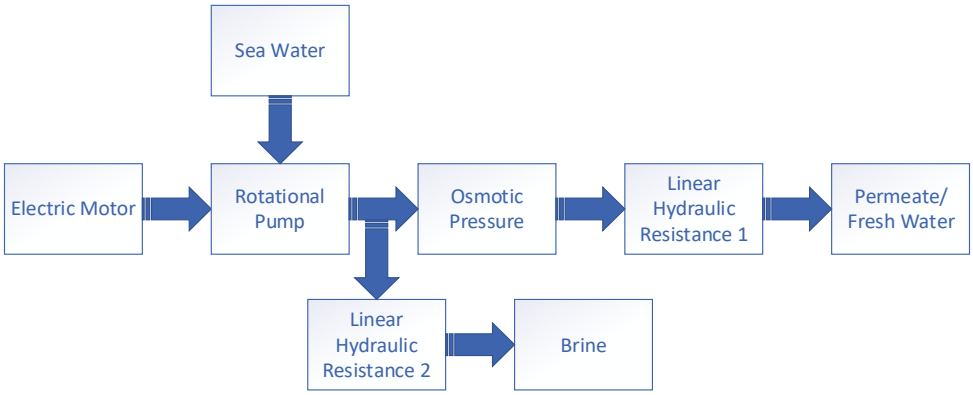

Figure 2.6: Flow chart of a RO membrane with hydraulic flow and pressure monitoring

The electrical analogue of the RO membrane model in Figure 2.7 includes the total flow rate source, linear hydraulic resistance-1 (LHR1), linear hydraulic resistance-2 (LHR2) and osmotic pressure element/diode. Equations (4) and (5) were used to identify LHR1 and LHR2 from the OSWEC DS, where I_{in} represents total flow rate, V_D denotes osmotic pressure, V_A signifies operating pressure of the source (I_{in}), and n indicates recovery ratio.

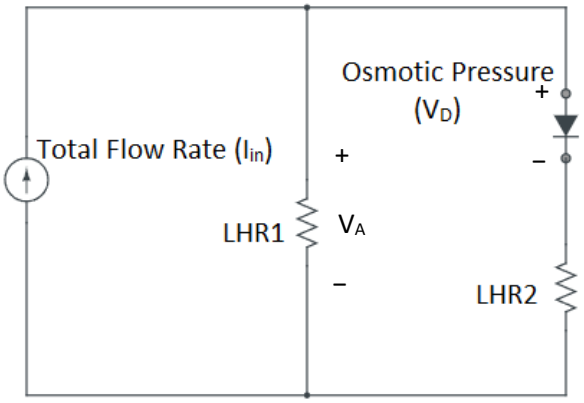

Figure 2.7: Electrical analogue of RO membrane process

$$LHR_1 = \frac{V_A}{I_{in} \times (1-n)} \qquad (4)$$

$$LHR_2 = \frac{V_A - V_D}{n \times I_{in}} \qquad (5)$$

On the other hand, in Figure 2.8, the speed or flow rate controller of the electrical motor controls the power generation to drive the motor, which in turn powers the pump of the RO system (see also Figure A.3 in Appendix B). To regulate the motor speed, proportional and integral constants were tuned for the proper fluid system dynamics. When the total flow rate reference is divided by the displacement ratio of the pump, the proper speed reference is obtained.

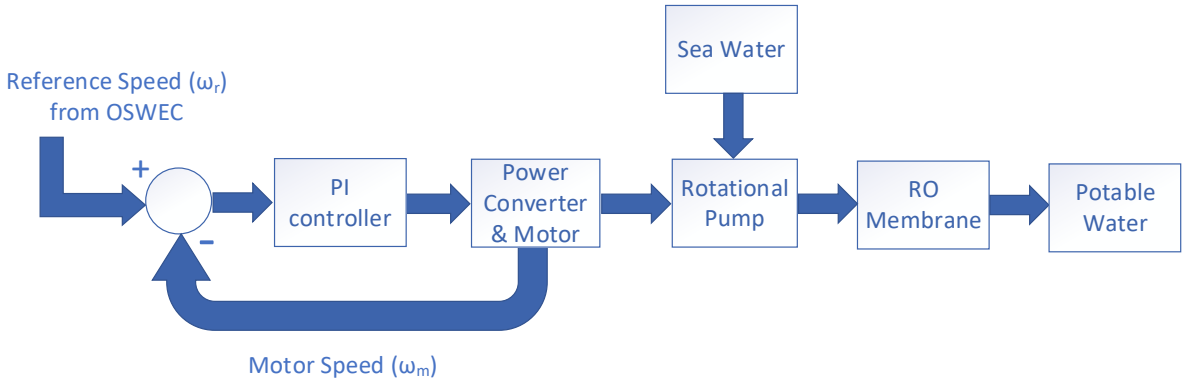

Figure 2.8: Electrical DS with speed control and reverse osmosis membrane

2.2.4 Analysis with different WEC geometry (slider crank radius and arm length):

Different values of the slider crank radius, ranging from 1.1 m to 2 m, were experimented with. Additionally, the arm length was varied between 3 m and 10 m. Based on these experiments, the optimum values of radius and arm length to achieve maximum power output were determined.

2.2.5 Description of testing with 7 different geographical locations:

Table 3.1: The Set of Centroids, and the Associated Power, Steepness, Adjusted Weights, Weighted Power, and Percent of Average Annual Power

Location	**Wave Period, T_p (s)**	**Wave Height, $H_s(m)$**	**Power Flux**	**Steep^{-1} $\lambda T_p / H_s$**	**Scaling Factor**	**Weighted Power Flux (KW/m)**	**Contrib. to AAP Flux %**
Glacier Bay, AK	7.31	2.34	16.7	35.6	0.243	4.07	11
	9.86	2.64	29.0	57.5	0.332	9.62	27
	11.52	5.36	141.1	38.6	0.075	10.59	30
	12.71	2.05	23.1	122.4	0.200	4.61	13
	15.23	5.84	233.5	60.4	0.024	5.61	16
	16.50	3.25	79.8	124.9	0.012	1.00	3
Aberdeen, WA	7.31	2.34	16.7	35.6	0.137	2.29	7
	9.86	2.64	29.0	57.5	0.277	8.03	25
	11.52	5.36	141.1	38.6	0.041	5.82	18
	12.71	2.05	23.1	122.4	0.338	7.80	24
	15.23	5.84	233.5	60.4	0.022	5.19	16
	16.50	3.25	79.8	124.9	0.045	3.56	11
Camp Rilea, OR	7.31	2.34	16.7	35.6	0.155	2.60	7
	9.86	2.64	29.0	57.5	0.307	8.88	23
	11.52	5.36	141.1	38.6	0.056	7.88	20
	12.71	2.05	23.1	122.4	0.344	7.94	20
	15.23	5.84	233.5	60.4	0.037	8.63	22
	16.50	3.25	79.8	124.9	0.042	3.35	9
Newport, OR	7.31	2.34	16.7	35.6	0.175	2.93	8
	9.86	2.64	29.0	57.5	0.268	7.77	20
	11.52	5.36	141.1	38.6	0.058	8.12	21
	12.71	2.05	23.1	122.4	0.295	6.80	18
	15.23	5.84	233.5	60.4	0.034	8.00	21
	16.50	3.25	79.8	124.9	0.054	4.29	11
	7.31	2.34	16.7	35.6	0.207	3.47	11
	9.86	2.64	29.0	57.5	0.230	6.67	21
	11.52	5.36	141.1	38.6	0.012	1.64	5

Bodega, CA	12.71	2.05	23.1	122.4	0.466	10.76	34
	15.23	5.84	233.5	60.4	0.016	3.85	12
	16.50	3.25	79.8	124.9	0.064	5.08	16
Lompoc, CA	7.31	2.34	16.7	35.6	0.152	2.54	8
	9.86	2.64	29.0	57.5	0.270	7.81	25
	11.52	5.36	141.1	38.6	0.014	2.00	6
	12.71	2.05	23.1	122.4	0.391	9.03	29
	15.23	5.84	233.5	60.4	0.010	2.24	7
	16.50	3.25	79.8	124.9	0.095	7.61	24
Oahu, HI	7.31	2.34	16.7	35.6	0.328	5.49	33
	9.86	2.64	29.0	57.5	0.245	7.09	42
	11.52	5.36	141.1	38.6	0.001	0.10	1
	12.71	2.05	23.1	122.4	0.133	3.07	18
	15.23	5.84	233.5	60.4	0.000	0.03	0
	16.50	3.25	79.8	124.9	0.013	1.06	6

The study analyzed wave energy potential and device performance in several locations along the U.S. Pacific West Coast, as well as in Hawaii and Alaska, focusing on both large-scale energy production and early market opportunities [24]. The selected sea states represent a variety of wave climates, with locations chosen for their good wave conditions, wide geographic spread, long-term data availability, and potential for future wave energy projects. Table 3.1 shows key wave parameters like wave height, period, and power flux, as well as additional factors that describe wave energy density and variability. Locations like Newport, OR, and Bodega, CA, stand out for their high energy potential, while Glacier Bay, AK, and Oahu, HI, are promising for smaller, early-stage projects. Overall, the results highlight the diversity of wave conditions across these areas and provide valuable insights for designing and deploying wave energy systems. The table provides detailed wave energy data for several locations along the U.S. Pacific West Coast, as well as in Alaska and Hawaii. It includes important parameters such as wave peak period (T_p), significant wave height (H_s), and wave power flux, which indicate the energy available at each site. Additional metrics like steepness and the parameter ($\lambda T_p/H_s$) help describe the wave conditions and their suitability for energy extraction. The table also calculates the weighted power

flux contribution of each sea state to the Average Annual Power (AAP) flux, showing how much each wave condition influences the overall energy potential of a location. High-energy sites like Newport, OR, and Bodega, CA, contribute significantly to the AAP flux, while Glacier Bay, AK, and Oahu, HI, offer opportunities for early-stage projects despite smaller contributions. This table is critical for understanding the variability and potential of wave energy across different regions.

CHAPTER 3: RESULTS AND DISCUSSION

3.1 Wave-Powered Desalination System (WPDS) Performance Analysis for OSWEC

The wave-to-water model was employed to evaluate the WPDS under various ocean states. Results demonstrated that the system's performance is highly influenced by both the flow rate and water salinity. As illustrated in Fig. 3.1, an optimal piston size can be determined for a specific number of membranes to maximize permeate flow. Notably, increasing the number of membranes improved the PFR up to a certain threshold, beyond which the permeate flow per membrane significantly declined. This trend suggests a limit to how much increasing membrane numbers contributes to system efficiency. Using this OSWEC system, desired flow rates and corresponding speed references were obtained to be used in the electrical desalination process.

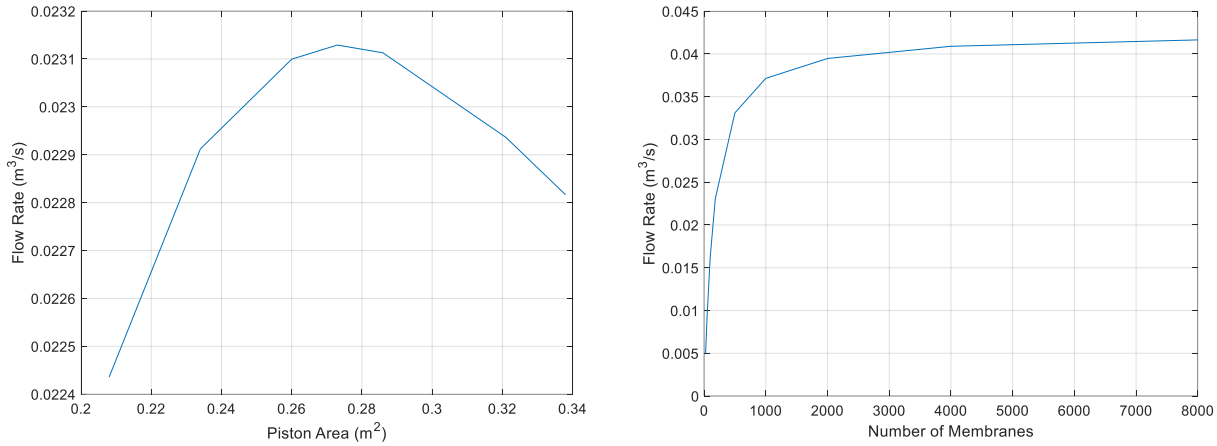

Figure 3.1: Annual weighted average permeate flow rate vs piston area (left) and number of membranes (right)

Altering the number or type of membranes in the OSWEC desalination system can tamper with the mechanical setup, requiring adjustments to maintain optimal performance. For example, increasing the number of membranes may affect flow dynamics and pressure requirements, necessitating modifications to pumps, piping, and structural housings. Such

changes could also influence the spatial layout, requiring redesigns to accommodate the new configuration and ensure accessibility for maintenance. These adjustments highlight the interconnectedness of the system, where even small alterations to the membrane setup can have a significant impact on the mechanical design and operation.

3.2. Slider Crank Mechanism and Generator Power Output for RM3

For the electrical system powering the desalination process, the slider crank mechanism was analyzed. Figure 3.2 shows that the generator's power output is highly sensitive to changes in crank radius, while arm length exhibited less influence. This sensitivity should guide future designs to focus on optimizing crank radius for maximizing energy conversion efficiency. In this research, the optimal crank radius was determined to be 1.5 meters, with an arm length of 7 meters.

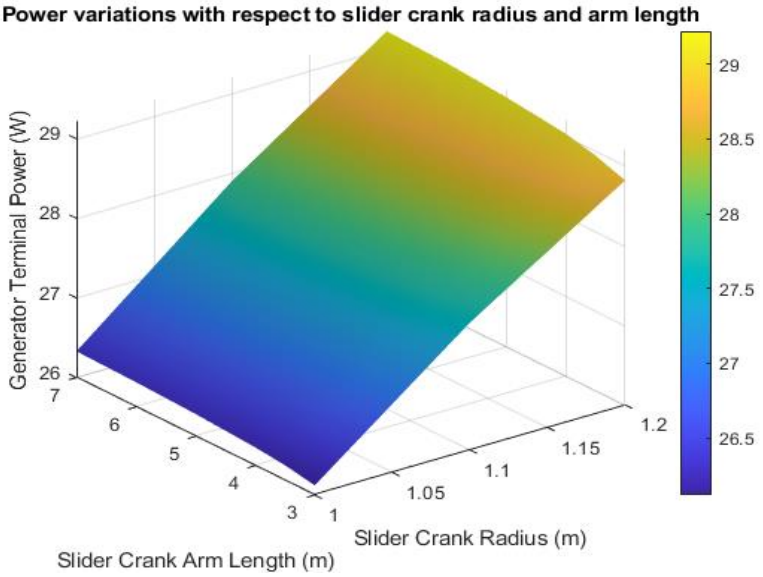

Figure 3.2: WEC power vs. slider crank radius and arm length

3.3 Desalination variables and supercapacitor integration in RM3 enhance performance

Figure 3.3-3.14 illustrates the performance of key desalination system (DS) variables, including permeate flow rate (PFR), pump motor power, and the state of charge (SOC) of the integrated supercapacitor, across sea states SS1 to SS6. The figures also highlight the fluctuations

of PFR for the Oscillating Surge Wave Energy Converter (OSWEC) over time, reflecting the influence of varying sea states. The system achieves stable permeate flow rates, with recovery ratios of 19.1%, 22.7%, 27%, 18.7%, 27%, and 24.8% for SS1, SS2, SS3, SS4, SS5, and SS6, respectively, aligning well with expectations in reference to the OSWEC benchmark system. As shown in the figures, the PFR in the OSWEC exhibits significant fluctuations, while the RM3 demonstrates much more stable performance. Furthermore, the RM3 shows promising results in both the power drawn from the motor and the state of charge of the supercapacitor. The integration of the supercapacitor and the tuning of the PI controller have contributed to the smoother and more stable operation of the RM3 system.

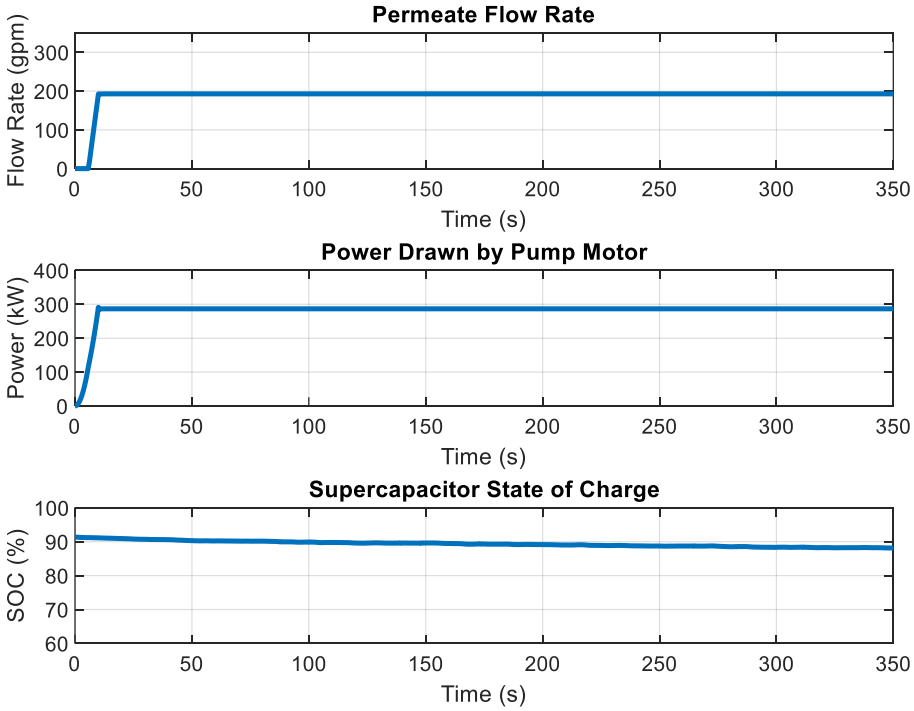

Figure 3.3: Electrically powered DS variables (permeate flow rate, power drawn by pump motor and SC state of charge) for the RM3 (SS1)

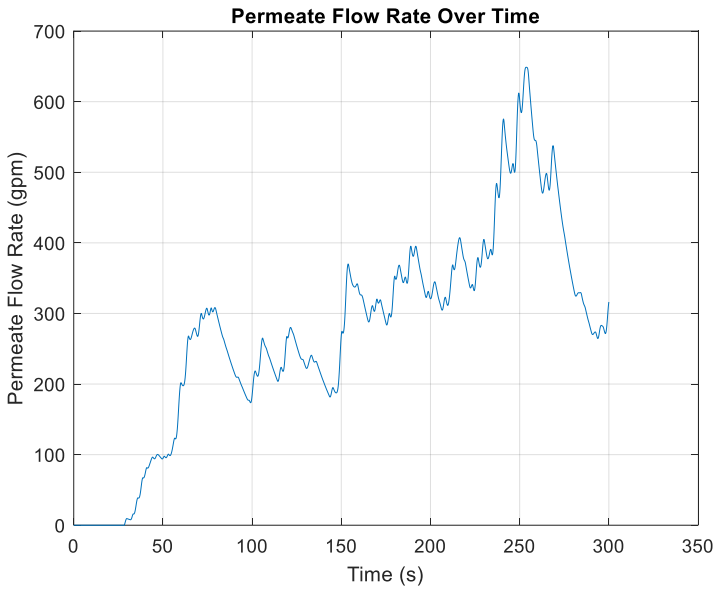

Figure 3.4: Mechanically powered DS PFR over time for the OSWEC (SS1)

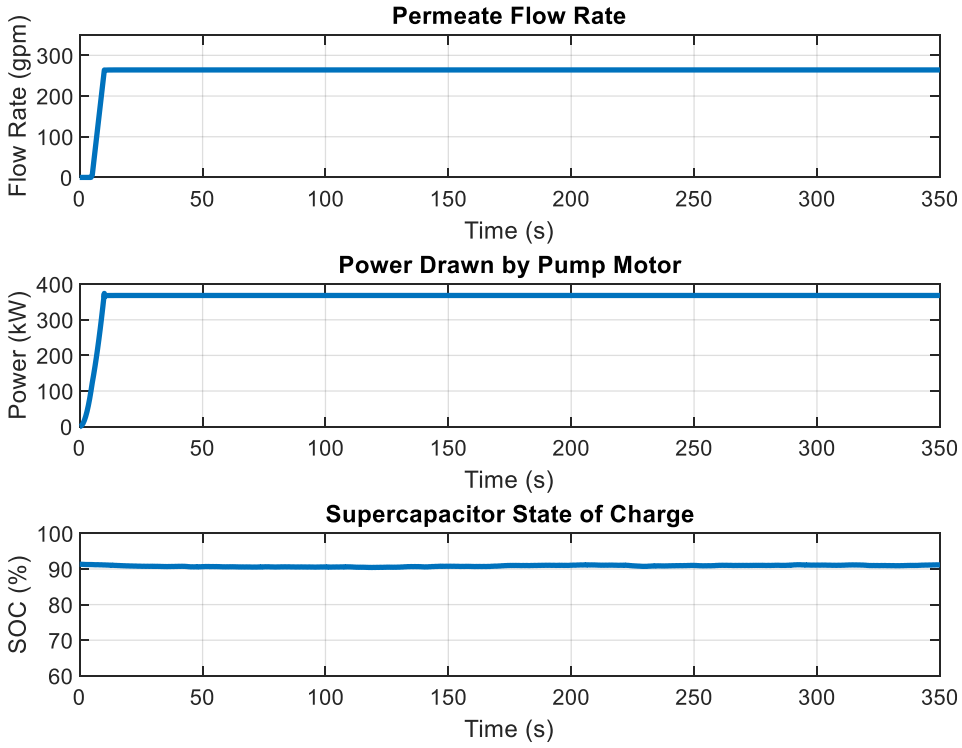

Figure 3.5: Electrically powered DS variables (permeate flow rate, power drawn by pump motor and SC state of charge) for the RM3 (SS2)

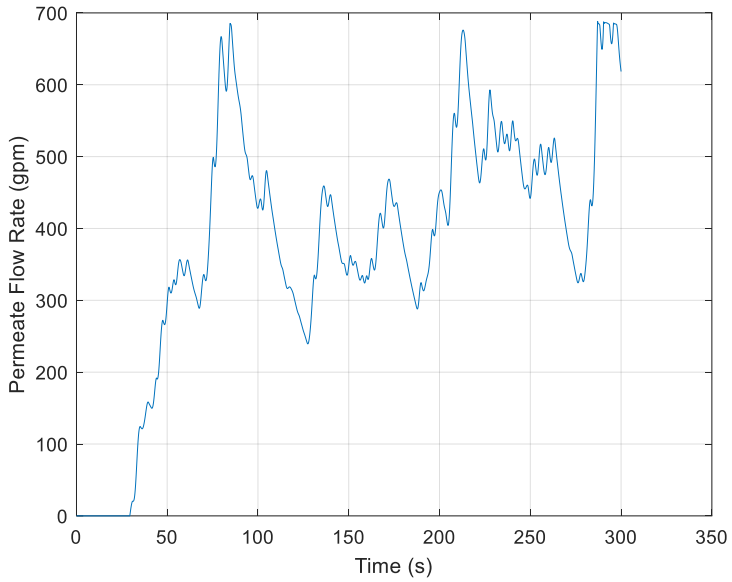

Figure 3.6: Mechanically powered DS PFR over time for the OSWEC (SS2)

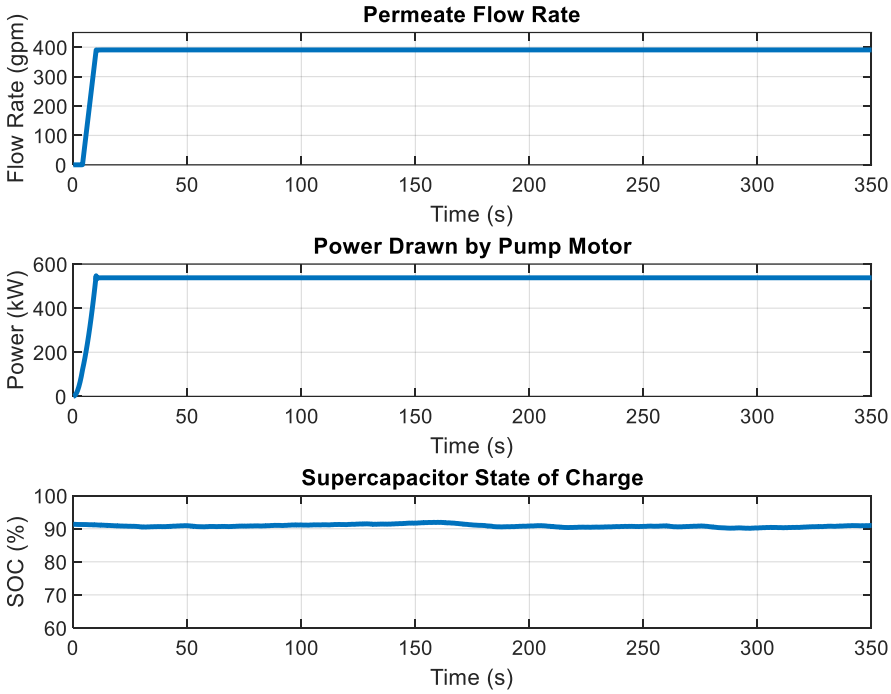

Figure 3.7: Electrically powered DS variables (permeate flow rate, power drawn by pump motor and SC state of charge) for the RM3 (SS3)

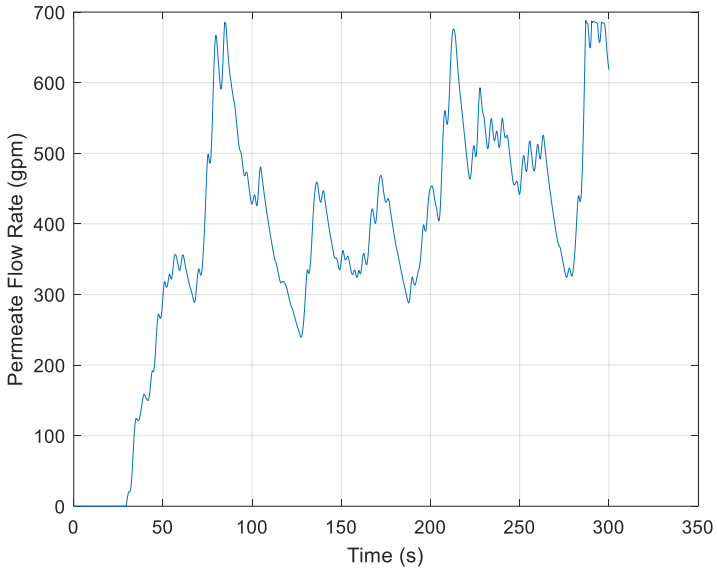

Figure 3.8: Mechanically powered DS PFR over time for the OSWEC (SS3)

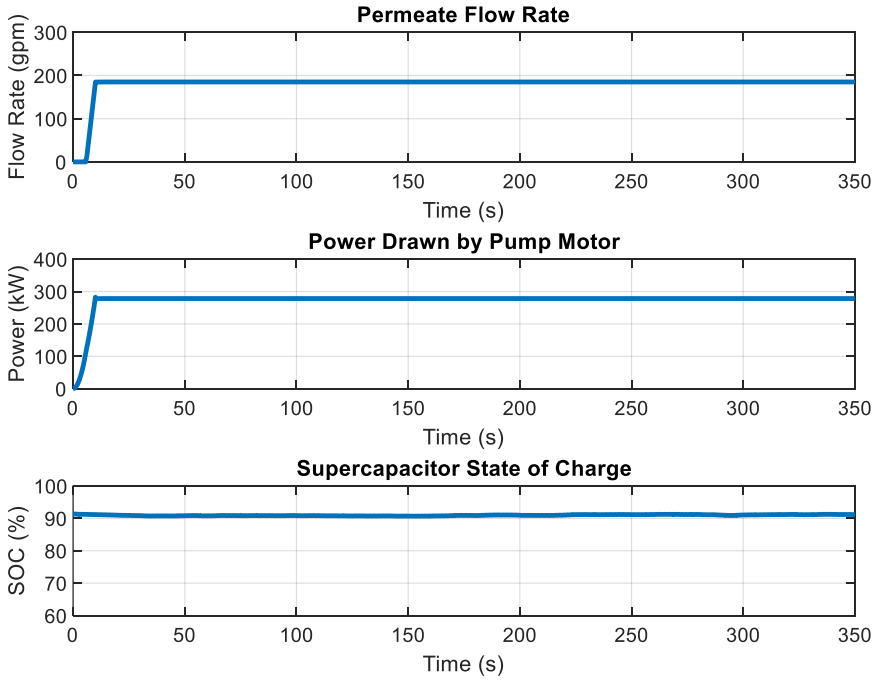

Figure 3.9: Electrically powered DS variables (permeate flow rate, power drawn by pump motor and SC state of charge) for the RM3 (SS4)

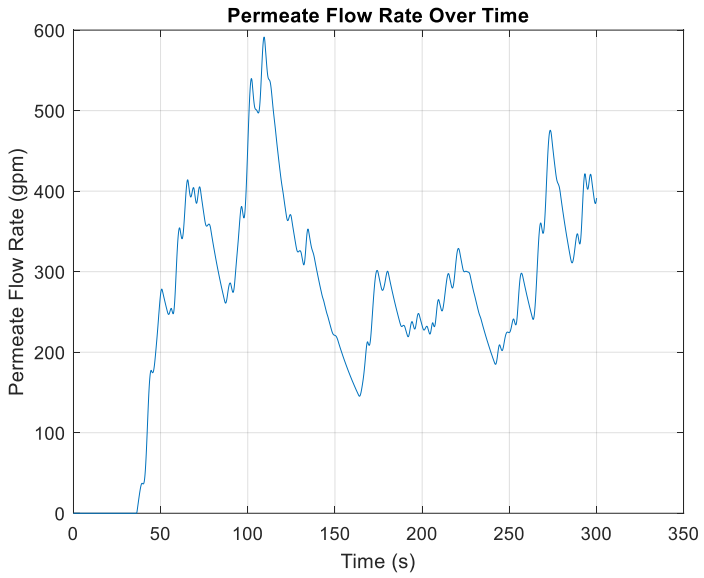

Figure 3.10: Mechanically powered DS PFR over time for the OSWEC (SS4)

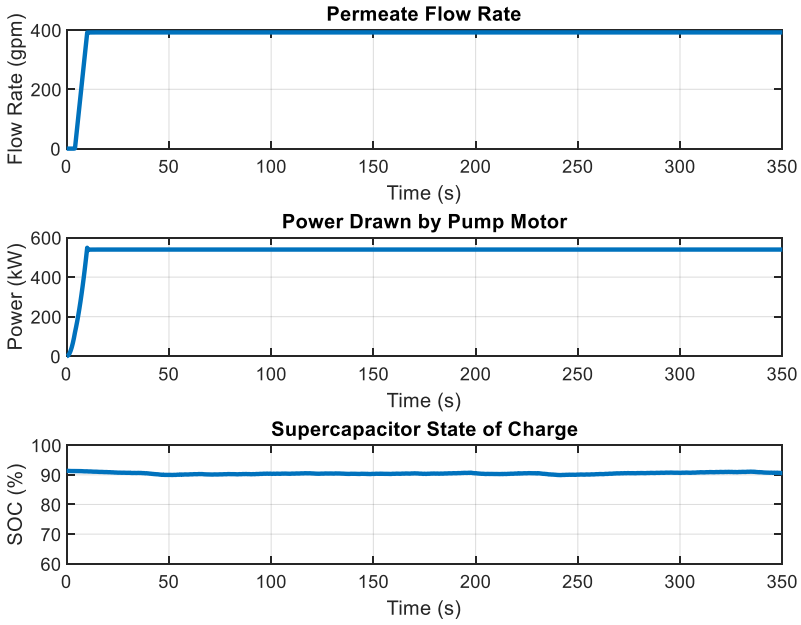

Figure 3.11: Electrically powered DS variables (permeate flow rate, power drawn by pump motor and SC state of charge) for the RM3 (SS5)

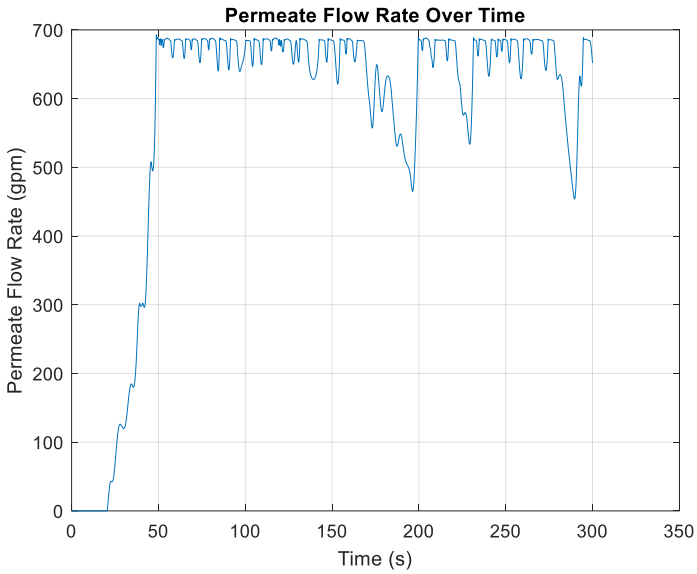

Figure 3.12: Mechanically powered DS PFR over time for the OSWEC (SS5)

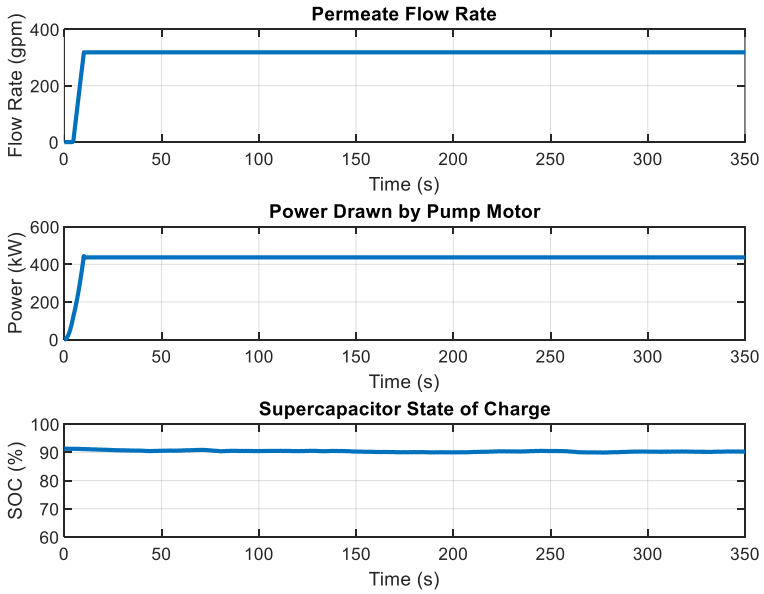

Figure 3.13: Electrically powered DS variables (permeate flow rate, power drawn by pump motor and SC state of charge) for the RM3 (SS6)

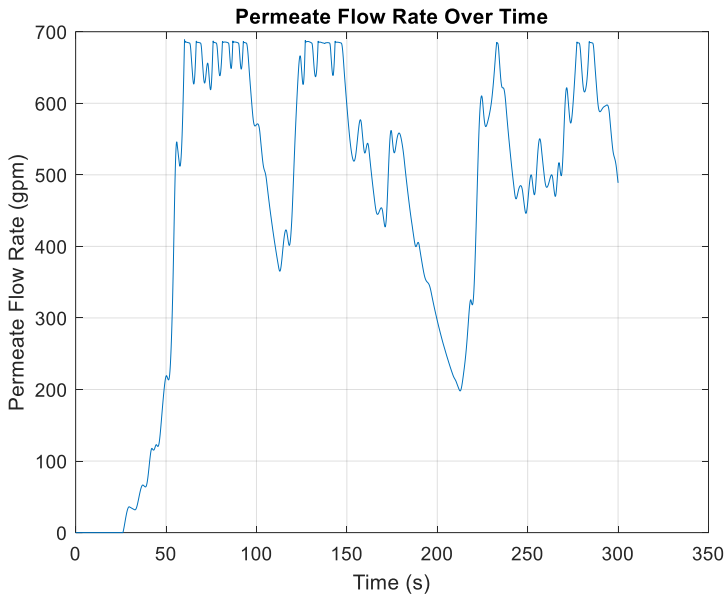

Figure 3.14: Mechanically powered DS PFR over time for the OSWEC (SS6)

The pump motor power stabilizes after an initial fluctuation period, indicating that proper system tuning supports dynamic and steady-state operation. Meanwhile, the SOC curve exhibits a smooth trend, demonstrating efficient energy management. The supercapacitor integration effectively buffers wave energy fluctuations, ensuring stable operation without the need for additional components like pressure relief valves and accumulators, as used in the OSWEC system. As can be in Figure 3.3-3.14, the RM3 based electrical desalination system showed a comparable performance to the OSWEC based mechanical desalination system given the system ratings. This conclusion is justified based on the relatively steady SOC level in the supercapacitor throughout the simulation.

3.4 Performance Comparison Between OSWEC and RM3 Models

The permeate flow rate for the RM3 system was calculated based on the scaled power output of the Oscillating Surge Wave Energy Converter (OSWEC) model. The OSWEC benchmark generates a rated power of 450 kW, while the RM3 system generates 286 kW. To account for this difference, a scaling factor of 0.6 was applied, derived from the ratio of RM3's

rated power to OSWEC's rated power. The mean permeate flow rate (MPF) and mean total flow rate (MTF) were obtained from OSWEC benchmark simulations, while the recovery ratio (RR) represented the fraction of the total water flow converted into permeate. The PFR for each sea state was calculated using (6).

$$PFR = MPF \times MTF \times RR \qquad (6)$$

Table 3.2 demonstrate the theoretical results of PFR (gpm) for SS1 to SS6 which are done using (6). It ranged from 185 gpm to 391 gpm, reflecting variations in wave energy and system performance. These findings aligned quite well with the simulation values. Utilizing the wave-to-water model, the performance of the WPDS was also evaluated under six selected sea states, representing different deployment conditions along the USA West Coast [24]. As shown in Table 3.3, the system yielded a PFR ranging from 155 to 225 gpm, offering significant insights into the impact of flow rate variations on the DS system performance.

Table 3.2: PFR Based on Theoretical Calculation

Sea States	**PFR (m^3/s)**	**PFR(gpm)**
SS1	0.0122	193
SS2	0.0167	264
SS3	0.0245	391
SS4	0.0117	185
SS5	0.0246	391
SS6	0.0200	318

Table 3.3: PFR in Various Locations Along USA West Coast

Location	**PFR (m^3/s)**	**PFR (gpm)**
Glacier Bay, AK	0.0135	214
Aberdeen, WA	0.0119	189
Camp Rilea, OR	0.0141	224
Newport, OR	0.0133	211
Bodega, CA	0.0137	217
Lompoc, CA	0.0135	214
Oahu, HI	0.0099	157

To sum up, it can be said that the RM3 system offers notable advantages over the OSWEC system, particularly in its ability to capture power from all directions. In contrast, the OSWEC system is limited to harnessing energy from a single direction, making it less adaptable to varying wave conditions. This directional limitation renders the OSWEC system less suitable for regions like North Carolina, where wave patterns can be diverse and multidirectional. Moreover, The RM3 demonstrates greater mooring flexibility compared to the OSWEC in locations such as the North Carolina (NC) coastal areas. This flexibility arises from RM3's point-absorber design, which relies on a floating buoy tethered to the seabed. This configuration allows it to adapt to a wider range of wave conditions, water depths, and seabed compositions commonly found along the NC coastline. In contrast, OSWECs are typically fixed to the seabed and operate optimally in shallower waters with consistent wave surges. Their fixed design limits adaptability in areas with varying bathymetry and tidal ranges like those in NC coastal waters. The RM3's mooring system can accommodate more dynamic wave-energy conditions and varying depths, making it a potentially more versatile choice for such environments.

CHAPTER 4: CONCLUSION AND FUTURE WORK

The current study highlights the potential of both mechanically and electrically powered DS, with a focus on optimizing performance through system design and integration. Mechanically powered systems demonstrate the importance of selecting an optimal piston size as well as membrane quantity to maximize permeate flow with some fluctuations, while electrically powered systems, utilizing WECs coupled with advanced control algorithms and RO processes, show promise in harnessing wave energy to produce potable water at a steady flow rate. Future research should aim to refine control algorithms, improve system designs, and explore the integration of other RES to enhance reliability and scalability. Additionally, investigating cost optimization related to membrane utilization will be crucial in maximizing the economic viability of the desalination process. Future work also includes optimizing supercapacitor size for the economic validity of the electrical desalination system. This work contributes to advancing renewable energy applications in water production, supporting sustainable development goals, and ensuring a resilient freshwater supply amidst global water scarcity challenges.

REFERENCES

[1] Naddeo V. One planet, one health, one future: the environmental perspective. Water Environ Res 2021;93:1472–5. https://doi.org/10.1002/wer.1624.

[2] Cavagnaro RJ, Copping AE, Green R, Greene D, Jenne S, Rose D, et al. Powering the blue economy: progress exploring marine renewable energy integration with ocean observations. Mar Technol Soc J 2020;54:114–25. https://doi.org/10.4031/ MTSJ.54.6.11.

[3] Gain AK, Giupponi C, Wada Y. Measuring global water security towards sustainable development goals. Environ Res Lett 2016:11. https://doi.org/10.1088/1748-9326/11/12/124015.

[4] Hanak E, Mount J, Chappelle C, Lund J, Medellín-Azuara J, Moyle P, et al. What if California's drought continues? Vol. 29. San Francisco; 2015.

[5] Lin S, Veerapaneni S. Emerging investigator series: toward the ultimate limit of seawater desalination with mesopelagic open reverse osmosis. Environ Sci Water Res Technol 2021;7:1212–9. https://doi.org/10.1039/d1ew00153a.

[6] Slocum AH, Haji MN, Trimble AZ, Ferrara M, Ghaemsaidi SJ. Integrated pumped hydro reverse osmosis systems. Sustain Energy Technol Assess 2016;18:80–99. https://doi.org/10.1016/j.seta.2016.09.003.

[7] M.M. Mekonnen, A.Y. Hoekstra, Four billion people facing severe water scarcity, Sci. Adv. 2 (2016) 1–6, http://dx.doi.org/10.1126/sciadv.1500323.

[8] Q. Chen, Y. Liu, C. Xue, Y. Yang, and W. Zhang, "Energy self-sufficient desalination stack as a potential fresh water supply on small islands," *Desalination*, vol. 352, pp. 26-35, Feb. 2015. https://doi.org/10.1016/j.desal.2014.12.010

[9] UN-Water, Water for a sustainable world, The United Nations World Water Development Report 2015, 2015, http://dx.doi.org/10.1016/S1366-7017(02)00004-1.

[10] J. Mi, X. Wu, J. Capper, X. Li, A. Shalaby, R. Wang, S. Lin, M. Hajj, and L. Zuo, "Experimental investigation of a reverse osmosis desalination system directly powered by wave energy," Applied Energy, vol. 343, 2023, Art. no. 121194. Available: https://doi.org/10.1016/j.apenergy.2023.121194

[11] J. Leijon and C. Boström, "Freshwater production from the motion of ocean waves – A review," Desalination, vol. 435, pp. 161-171, 2018. Available: https://doi.org/10.1016/j.desal.2017.10.049

[12] Y.-H. Yu and D. Jenne, "Numerical modeling and dynamic analysis of a wave-powered reverse-osmosis system," J. Mar. Sci. Eng., vol. 6, p. 132, 2018. Available: https://doi.org/10.3390/jmse6040132

[13] R. Suchithra, T. K. Das, K. Rajagopalan, A. Chaudhuri, N. Ulm, M. Prabu, A. Samad, and P. Cross, "Numerical modelling and design of a small-scale wave-powered desalination system," Ocean Eng., vol. 256, p. 111419, 2022. [Online]. Available: https://doi.org/10.1016/j.oceaneng.2022.111419

[14] J. Mi, X. Wu, J. Capper, X. Li, A. Shalaby, U. Chung, R. Datla, M. Hajj, and L. Zuo, "Ocean Wave Powered Reverse Osmosis Desalination: Design, Modeling and Test Validation," IFAC-PapersOnLine, vol. 55, no. 37, pp. 782-787, 2022. Available: https://doi.org/10.1016/j.ifacol.2022.11.277

[15] J. Leijon, D. Salar, J. Engström, M. Leijon, and C. Boström, "Variable renewable energy sources for powering reverse osmosis desalination, https://doi.org/10.1016/j.desal.2020.114669

[16] J. Leijon, J. Engström, M. Göteman, and C. Boström, "Desalination and wave power for freshwater supply on Gotland," Energy Strategy Reviews, vol. 53, p. 101404, 2024. Available: https://doi.org/10.1016/j.esr.2024.101404

[17] https://wec-sim.github.io/WEC-Sim/ (accessed on 5 October 2024).

[18] Yu, Y.H.; Lawson, M.; Ruehl, K.; Michelen, C. Development and Demonstration of the WEC-Sim Wave Energy Converter Simulation Tool. In Proceedings of the 2nd Marine Energy Technology Symposium (METS'14), Seattle,WA, USA, 15–17 April 2014.

[19] Cummins,W. The Impulse Response Function and Ship Motions; Technical Report; David Taylor Model Basin (DTNSRDC):Washington, DC, USA, 1962.

[20] Van't Hoff, J. Hydrodynamic Modelling of the Oscillating Wave Surge Converter. Ph.D. Thesis, The Queen's University of Belfast, Belfast, UK, 2009.

[21] DOW Water & Process Solutions. DOW Water Solution Design Software. Available online: https://www.dow.com/en-us/water-and-process-solutions/resources/design-software (accessed on 5 October 2024).

[22] https://tethys-engineering.pnnl.gov/signature-projects/rm3-wave-point-absorber

[23] H. B. Karayaka, Y.-H. Yu, and E. Muljadi, "Investigations into Balancing Peak-to-Average Power Ratio and Mean Power Extraction for a Two-Body Point-Absorber Wave Energy Converter," Energies, vol. 14, no. 12, p. 3489, 2021. Available: https://doi.org/10.3390/en14123489

[24] Bull, D, & Dallman, A. "Wave Energy Prize Experimental Sea State Selection." Proceedings of the ASME 2017 36th International Conference on Ocean, Offshore and Arctic Engineering. Volume 10: Ocean Renewable Energy. Trondheim, Norway. June 25–30, 2017. V010T09A025. ASME. https://doi.org/10.1115/OMAE2017-62675

APPENDIX

APPENDIX A

LHR1 and LHR2 calculation for SS1:

```
Iin =4.85e-06;

VD = 30e5;
n = 0.1918;
VA = 4.22e6;

LHR1 = VA/(Iin*(1-n))
LHR2 = (VA-VD)/(n*Iin)
```

LHR1 and LHR2 calculation for SS2:

```
Iin =5.62e-06;

VD = 30e5;
n = 0.2270;
VA = 4.67e6;

LHR1 = VA/(Iin*(1-n))
LHR2 = (VA-VD)/(n*Iin)
```

LHR1 and LHR2 calculation for SS3:

```
Iin =6.97e-06;

VD = 30e5;
n = 0.2705;
VA = 5.47e6;

LHR1 = VA/(Iin*(1-n))
LHR2 = (VA-VD)/(n*Iin)
```

LHR1 and LHR2 calculation for SS4:

```
Iin =4.77e-06;

VD = 30e5;
n = 0.1873;
VA = 4.17e6;

LHR1 = VA/(Iin*(1-n))
LHR2 = (VA-VD)/(n*Iin)
```

LHR1 and LHR2 calculations for SS5:

```
Iin =6.98e-06;

VD = 30e5;
n = 0.2708;
VA = 5.48e6;

LHR1 = VA/(Iin*(1-n))
LHR2 = (VA-VD)/(n*Iin)
```

LHR1 and LHR2 calculation for SS6:

```
Iin =6.20e-06;

VD = 30e5;
n = 0.2480;
VA = 5.02e06;

LHR1 = VA/(Iin*(1-n))
LHR2 = (VA-VD)/(n*Iin)
```

Power Outputs Calculation:

```
a=cumsum(-simout.data.*simout1.data*5e-4);a(end) % Generator Terminal Power
a=cumsum(-simout.data.*simout2.data*5e-4);a(end) % Back EMF Terminal Power
a=cumsum(simout4.data*5e-4);a(end) % Mechanical Power
```

Appendix B

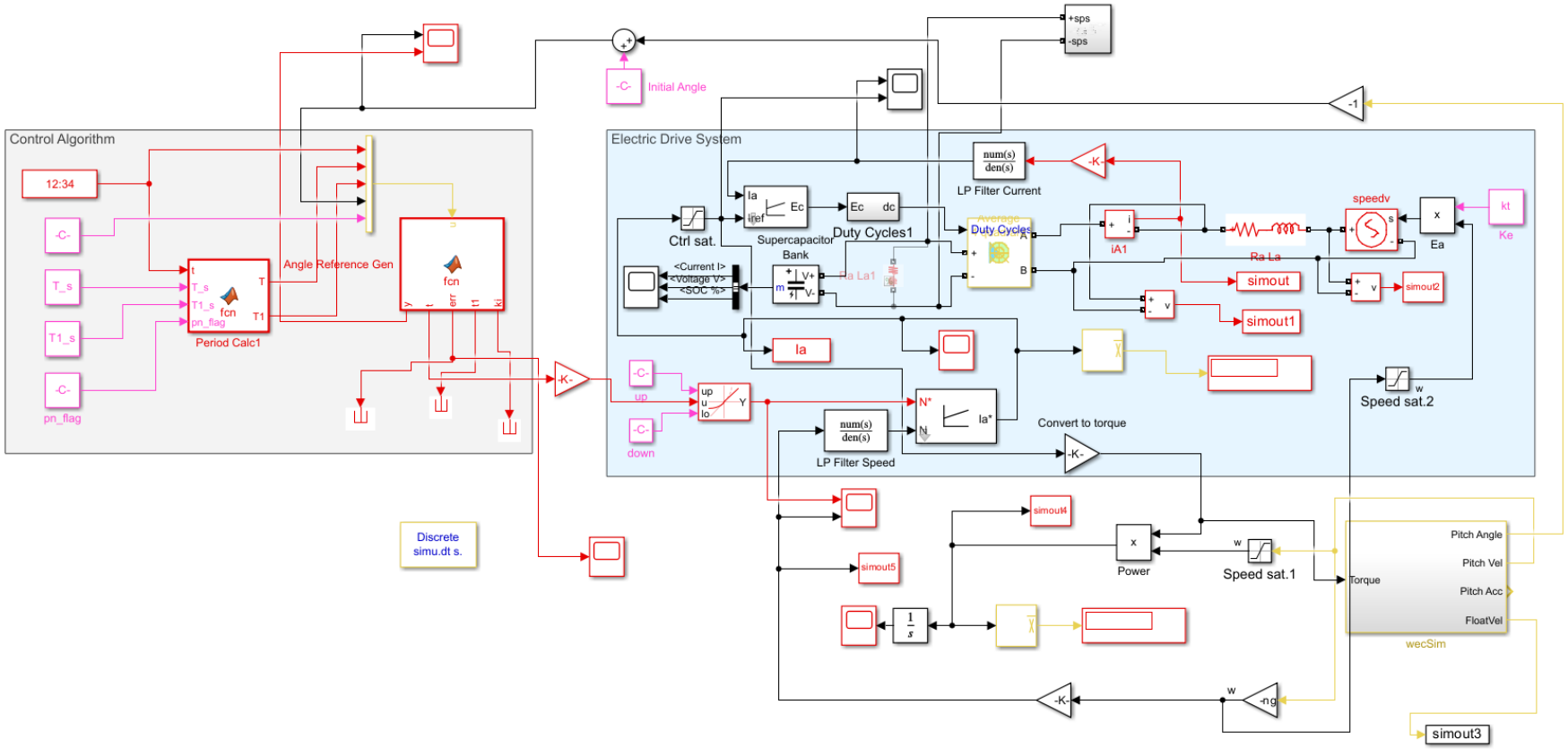

Figure A.1 Overall RM3 WEC system with the desalination plant

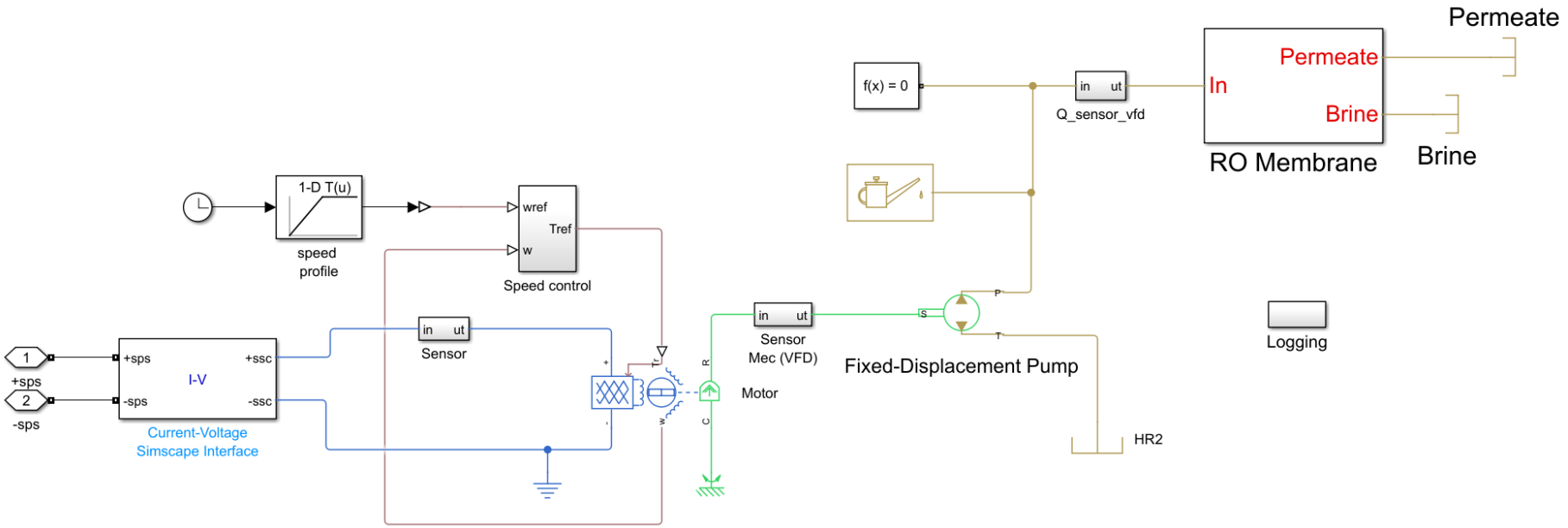

Figure A.2 The electrically driven desalination subsystem

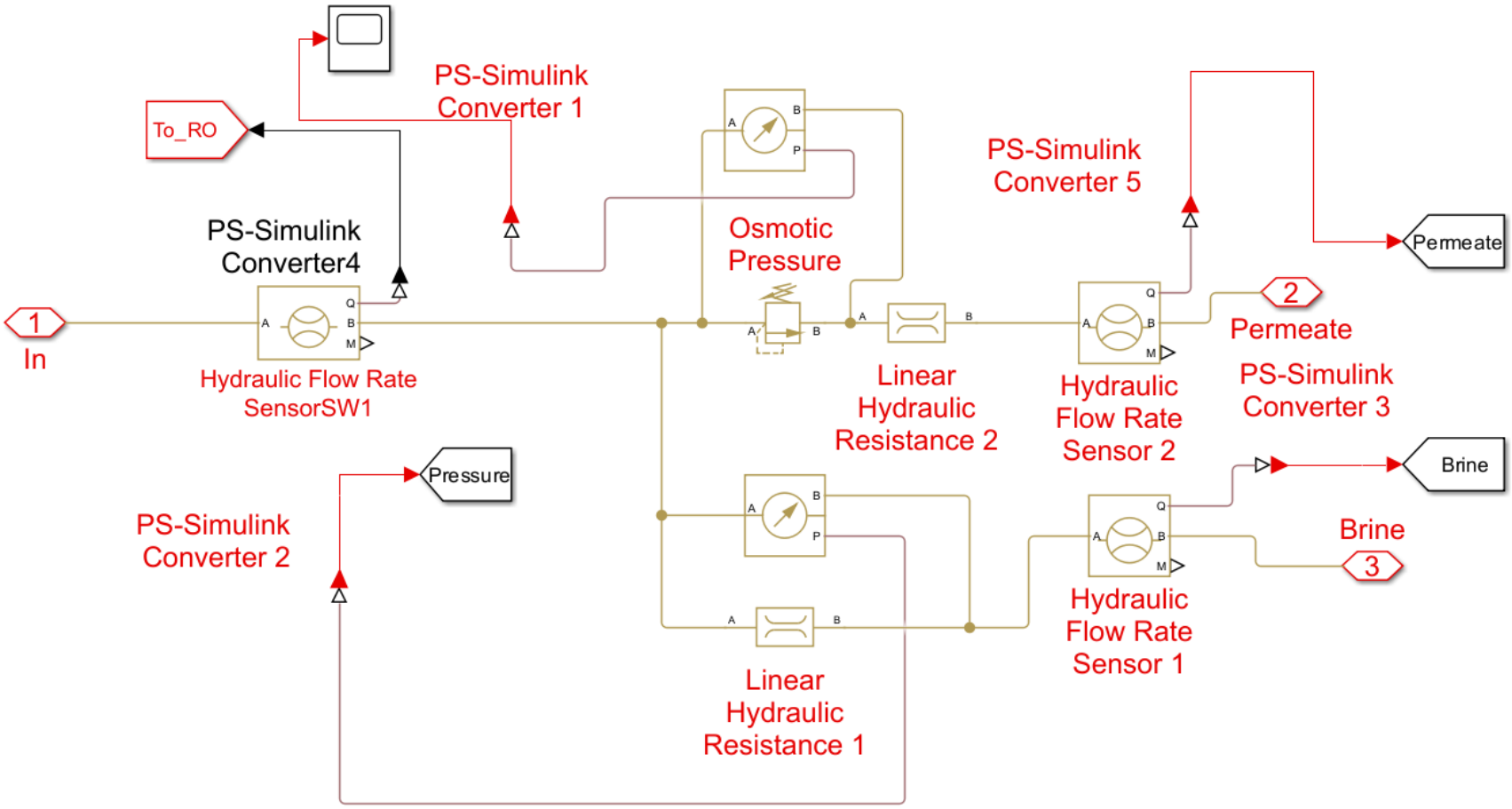

Figure A.3 RO membrane